Eötvös Loránd University
Faculty of Natural Sciences
Institute of Physics

Design and construction of a high-field superconducting septum magnet for the Future Circular Collider

3rd semester research report
Material Physics and Solid State Physics PhD Programme

Novák Martin István [1]
MTA Wigner Research Centre for Physics

Supervisor:
Barna Dániel [2]
MTA Wigner Research Centre for Physics

Consultant:
Horváth Ákos
ELTE TTK Department of Atomic Physics

2019.06.15.

[1] novak.martin@wigner.mta.hu
[2] barna.daniel@wigner.mta.hu

1 Introduction

The goal of this PhD work is to design, manufacture and assemble a working prototype of a passive high-field septum magnet which could be used in the beam injection and extraction system of the Future Circular Collider (FCC). For a more detailed introduction, I refer to [2, 6].

2 Achieved results in this semester

2.1 New septum magnet concept

I have spent the first month of the semester at CERN with the Magnet Design and Technology group, working on the assembly of a 2.2 m long CCT dipole corrector magnet. I had the chance to watch and help at different stages of the assembly of a CCT magnet starting from the winding of the formers to the soldering of the connections. I have noted many crucial steps during an assembly which are potential failure points. Also, the design of the SuShi septum was updated based on these observations. This experience will be extremely helpful when it comes to the assembly of the SuShi septum prototype at Wigner RCP.

Our group at Wigner RCP handed in an application for a new project called Heavy Ion Therapy Research Infrastructure (HITRI) which aims to conceptualize everything needed to build a medical accelerator, standardizing the development of hadron therapy centres for carbon and heavier ions. The task of our group would be to design a superconducting extraction/injection system for square-shaped accelerators with 4 m side length. These magnets do not have to reach very high fields, but they have to be compact. We have developed a 2D concept of an opposite-field septum magnet which could be a candidate for this purpose.
In the opposite field concept, the septum magnet has $\pm B_0$ magnetic field at the two sides of the septum. There are several benefits to this design:

- The peak field in the coils is reduced (which relaxes the requirements on the superconducting cables), since the same separation power is achieved by approximately with half the magnetic field, compared to a zero-high field arrangement
- There are no net forces acting on the septum blade

In the meantime a disadvantage of this arrangement is that it is not a single-cross device, so the field-quality becomes an important factor during the design. The desired magnetic field can be achieved by truncating an x-y dipole field generated by $J_z(\theta) = J_0 \cos(\theta)$. The idea of this truncation is described in [4]. Figure 2 shows the induction lines and the current. By setting the truncating current on the A-B-C line with proper direction, and eliminate the A-E-C part of the original current distribution, then the magnetic field in the shaded area will be zeroed and remains a pure dipole inside the A-B-C-F-A induction line. Superpostioning this current density with its horizontal mirror image will result in a field configuration with opposite signed B_0 at the two domains. Equation 1 describes such a current distribution.

$$J_z(s) = \begin{cases} -\frac{B_0}{\mu_0} & \text{if } 0 \text{ ¡ s ¡ } \frac{R\sqrt{3}}{2}, \text{ (B-C) line} \\ -\frac{B_0}{\mu_0}\left(2\cos(\varphi) + \frac{1}{2-2\cos(\varphi)}\right) & \text{if } \frac{R\sqrt{3}}{2} < s < S_{max} = R\cdot 120^\circ + R\frac{\sqrt{3}}{2} \text{ (C-D) line} \end{cases} \quad (1)$$

where

$$\varphi = \frac{s - R\sqrt{3}/2}{R} + 60^\circ \text{if } s > \frac{R\sqrt{3}}{2} \quad (2)$$

The placement of the wires was calculated in a simple Python code, where a mapping between the current density and the arc length parameter was determined, divided into smaller intervals, and the cables were placed into the centre of gravity of these intervals using $J(s)$ as a

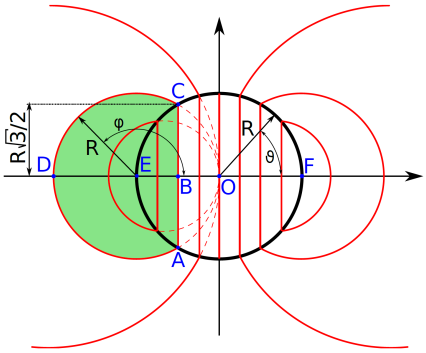

Figure 2: Illustration of the induction lines (red) of a $cos(\theta)$ sheet current distribution (thick black circle). The dashed lines show the extensions of the induction lines of the external domain to the interior of the current distribution

weighting function. A more detailed analysis can be found in [5]. The magnetic field of the magnet was composed of the vector potentials of wires taken as point sources (which is known in the analytical form) at their given place. The results are shown in Fig. 3 The magnetic field

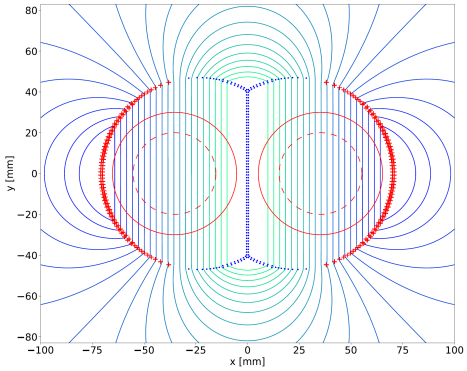

Figure 3: Results of the cable placement and magnetic field calculation. Red crosses: positive wires, Blue dots: negative wires, Lines: magnetic induction lines

distribution was multipole analyzed, and the magnet shows excellent field quality since every non-dipole multipole's magnitude is smaller than 1 unit.

2.2 Quench simulation framework

Since the adaptation of existing quench simulation codes[7] for the CCT SuShi is not straightforward, a custom simulation framework was developed entirely in COMSOL Multiphysics powered by its Java API. The framework can describe eddy current heating, quench back, strand-to-strand heat propagation, longitudinal quench propagation and helium cooling. The goals during the design were

- Be able to easily generate simulations for any kind of CCT-like coil shapes
- Minimize the necessary pre-calculations
- Solve the problem with a single software

- Be able to calculate the hotspot-temperature directly, not using adiabatic approximations

The model uses temperature-dependent material properties everywhere. These were taken from STEAM's[8] material library and [9]. It consists of components with different dimensions.

The cornerstone of the simulation is the assumption that due to the high heat conductivity of the aluminium every local hotspot diffuses quickly, and this does not raise the temperature of the aluminium significantly due to its large mass (compared to the strands). This allows to model only the 2D cross-section of the magnet.

The strands are described by 10 almost identical 1D components, each thermally coupled to its neighbours and the formers. A modified polar map is used to map the temperature distribution of a spar of a former into an auxiliary space where the temperature profile is given in Cartesian coordinates. In this auxiliary space, the radial dimension is integrated out then divided by the spar thickness resulting in a 1D temperature profile. This temperature profile is then used to generate $Q_{s,f} = h_{s,f} \cdot (T_{former1D} - T_s)$ where s is the index of the 1D strand component and $h_{s,f}$ is the heat rate between the former and the given strand. If a temperature of the strand is larger than the current sharing regime temperature, then a Joule heating is enabled at that place.

The coupling coefficients (heat rates) between the coils are calculated in two coupled 2D detailed model of the whole coil pack, including epoxy and Kapton insulation on the surface of the strands. In one of the coil pack models, the strand temperatures are constrained to have the maximal temperature of the corresponding 1D strand component, in the other, it is fixed to the minimal strand temperature. In both model the instantaneous heat transfer is calculated between the strands using

$$h_{ij}^{2D,max/min} = \frac{\oint_{\partial_{strand_j}} \mathbf{q} \cdot \mathrm{d}\mathbf{r}}{A \cdot (max/min(T_i) - max/min(T_j))} \tag{3}$$

The argument t for time dependence is suppressed for brevity. Then the coupling between of the ith strand to the jth is given by $Q_{ij}(x) = h_{ij}\left(T_j(x)\right) \cdot (T_i(x) - T_j(x))$ where $h_{ij}(T)$ is calculated as a linear interpolation between the minimal and maximal temperature coil pack components' result:

$$h_{ij}\left(T\right) = \frac{h_{ij}^{(2D,min} \cdot (max(T) - T) + h_{ij}^{(2D,max} \cdot (T - min(T))}{max(T) - min(T)} \tag{4}$$

The current in the 2D cross-section component and in the 10 1D components are driven by a system of ODEs, which describes the RL circuit model of the magnet with the coil as primary, and the formers as secondary coils. The inductance matrix is calculated from a 3D COMSOL model, with a simplified coil geometry. A summary with the upper mentioned coupling is shown in Fig. 4. A temperature dependent liquid helium cooling is applied on the inner boundary of the inner former and the outer boundary of the support tube. The following events happen during the simulation:

- The full coil current is flowing through all 1D components and drives the 2D cross-section.
- A small (but large enough to push that location into the current sharing regime) temperature disturbance is introduced at some position in one of the strand components.
- This disturbance starts to grow, raising the ohmic resistance of the strand (the 10 strands are soldered together serially), thus the voltage between the start and the end of the joined strands
- If the voltage rises above the quench detection threshold, and stays above for a certain amount of time (validation) then the ODE module is enabled and starts to ramp down the current in the 1D components and in the cross-section component

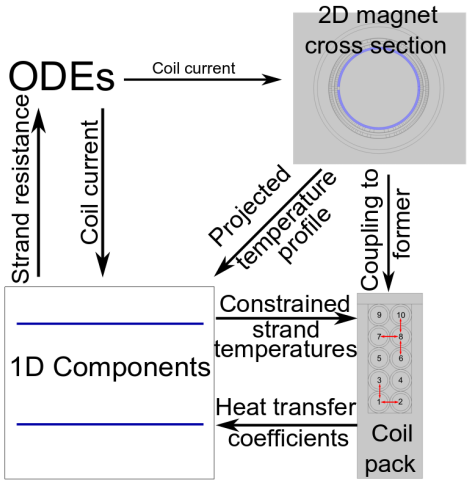

Figure 4: Summary of the quasi 3D quench simulation.

- This changing current induces currents in the conductive parts of the 2D cross-section component, which start to heat up the formers
- Due to the former-strand coupling this temperature profile of the former is soon present in the longitudinal temperature profile of the strands.
- As the strands close to the spar starts to heat up, they can heat their neighbours, so after a while, the upper strands will adopt this temperature profile too.
- This continues until the current ramped down to 0, then the simulation ends

The presence upper mentioned phenomenons were tested both individually and in a coupled way, and the results suggest that the simulation works correctly. Currently, it is in the phase of validation, and testing the acceptability of the neglections (like neglected rib heat transfer, and the feasibility of the linear interpolation of the heat rates, etc.). These tests have to be finished until the middle of February since I present this work at CERN at the second half of February, and I am planning to will write an article about this simulation framework, being the lead author.

3 Publications

D. Barna, M. Novák *Two-dimensional conceptual design of an iron-free opposite-field septum magnet* Nuclear Instruments and Methods in Physics Research (Reviewers accepted, under publishing)

D. Barna, M. Novák, K. Brunner, G. Kirby, B. Goddard, J. Borburgh, M. Atanasov. A. Sanz Ull, E. Renner, W. Bartmann, M. Szakaly, *Conceptual design of a high-field septum magnet using a superconducting shield and a canted-cosine-theta magnet* IEEE Transactions on Applied Superconductivity (Date of publication 31 May 2019.

D. Barna, G. Giunchi, K. Brunner, M. Novák, A. Német, C. Petrone, M. Atanasov, H. Bajas, J. Feuvrier, M. Pascal, *An MgB_2 superconducting shield prototype for the Future Circular Collider septum magnet* IEEE Transactions on Applied Superconductivity (Date of publication 31 May 2019.

D. Barna, M. Novak, K. Brunner, C. Petrone, M. Atanasov, J. Feuvrier, M. Pascal: *NbTi/Nb/Cu multilayer shield for the superconducting shield (SuShi) septum.* IEEE Transactions on Applied Superconductivity 29 (2019), 4900108 (Date of publication: 2 October 2018)

4 Conferences since last semester

- Presentation at the FCC Week 2019 conference in Brussels (2019.06.24-2019.06.28). Title: Status of the SuShi septum project

5 Education

Courses:

- Field theory, renormalization group and critical phenomenons
- Topological Insulators

References

[1] M. I. Novák, 1st semester PhD report 2019.

[2] M. I. Novák, 2nd semester PhD report 2019

[3] Status of the SuShi spetum project, M. I. Novák, FCC Week 2019 presentation

[4] F. Krienen, D. Loomba, W. Meng, (1989). The truncated double cosine theta superconducting septum magnet. Nuclear Inst. and Methods in Physics Research, A, 283(1), 5–12. https://doi.org/10.1016/0168-9002(89)91249-7

[5] D. Barna, M. Novák (2020). Two-dimensional conceptual design of an iron-free opposite-field septum magnet. Nuclear Instruments and Methods in Physics Research (Reviewers accepted, under publishing)

[6] Numerical and experimental study of superconducting magnetic shields for the construction of a high-field septum magnet, M. I. Novák, MSc thesis 2018.

[7] M. Mentink, J. Van Nugteren, F. Mangiarotti, M. Duda, G. Kirby (2018). Quench Behavior of the HL-LHC Twin Aperture Orbit Correctors. IEEE Transactions on Applied Superconductivity, 28(3), 1–6. https://doi.org/10.1109/TASC.2018.2794451

[8] L. Bortot, et. al. (2018). STEAM: A Hierarchical Cosimulation Framework for Superconducting Accelerator Magnet Circuits. IEEE Transactions on Applied Superconductivity, 28(3). https://doi.org/10.1109/TASC.2017.2787665

[9] P. Duthil, (2015). Material Properties at Low Temperature. https://doi.org/10.5170/CERN-2014-005.77